論文 95-6-6-4

A Double-Dwell Serial Code Acquisition for CDMA System

Hyung-Rae Park*, Bub-Joo Kang* Regular Members

CDMA 시스템을 위한 이중적분 직렬 동기획득 방식

正會員 朴 亨 來*, 康 法 周*

ABSTRACT

In this paper, the performance of the double-dwell serial code acquisition technique is analyzed in the CDMA forward link in frequency-selective Rayleigh fading channel.

A general expression for the mean acquisition time is derived by considering the multiple H_1 cells and 'returning' false alarm state. The detection and false alarm probabilities of the CDMA noncoherent demodulator are also derived analytically by taking into account the correlation between successive demodulator outputs within the period of post-detection integration. Based on the detection performance analysis and the expression for the mean acquisition time, the numerical performance evaluations of the code acquisition technique shall be performed to address the problems of selecting the design parameters for pilot signal acquisition in the CDMA forward link, illustrating the effects of post-detection integration and signal fading on code acquisition performance.

要 約

본 논문에서는 CDMA 순방향 링크에서의 이중적분 직렬동기획득 방식의 성능을 주파수 선택성 레일라이 페이딩 환경하에서 분석한다.

PN 칩 당 ℓ 번의 테스트를 수행하는 경우에 대해 다중 H_1 셀과 궤환 오경보('returning false alarm')를 고려한 평균동기획득시간을 유도하고 신호검출 및 오보확률을 복조기 출력의 상관관계를 고려하여 이론적으로 해석한다. 이를 기초로 CDMA 순방향 파일럿 신호의 동기획득을 위한 설계 파라미터의 설정방법과 후치적분 및 신호의 페이딩 특성에 따른 성능의 변화를 분석한다.

*한국전자통신연구소(ETRI)
이동통신 연구단 신호처리연구실
論文番號 : 94338-1125
接受日字 : 1994年 11月 25日

Ⅰ. Introduction

Recently, direct-sequence spread spectrum (DS-SS) technique has attracted much attention for mobile communication application, so called the code division multiple access (CDMA) system, which has been shown to have significant advantages over conventional analog FM system or time division multiple access (TDMA) system [1~3]. However, like other spread spectrum applications, the advantages of the CDMA system can be exploited only if the PN sequences of the local PN generator and incoming signal are synchronized within a fraction of one PN chip. The code synchronization in spread spectrum techniques consists of two steps, code acquisition (coarse alignment) and code tracking (fine alignment), of which the former is dealt with in this paper.

The serial search technique with fixed dwell time [4~7] is widely used for pilot signal acquisition in the CDMA forward link due to its advantage in implementation and high acquisition performance. The serial search technique can be divided into the single-dwell and multiple(mostly double)-dwell techniques, of which the latter is most popular. While most of the code acquisition techniques employ an active correlator for despreading incoming signal, they can be also designed by using the matched filter correlator (or passive correlator) [4,8,9] for fast code acquisition. Yet, since this technique requires a matched filter with large time-bandwidth product which makes a hardware complicated, it is not widely accepted in real applications. A further detailed classification can be found in [10].

The performance of the double-dwell serial code acquisition technique is analyzed in the CDMA forward link in frequency-selective Rayleigh fading channel by taking the mean acquisition time as a performance measure. So far, the performances of the code acquisition techniques have been discussed mostly with the assumption that there is a single H_1 cell within the H_1 region. However, since in practice, multiple cells belong to the H_1 region in the case of ι-hypothesis tests per PN chip, the single H_1 cell approach shows the mean acquisition time significantly longer than as it would be. A general expression for the mean acquisition time is therefore derived by considering the multiple H_1 cells and 'returning' false alarm state.

Although the expression derived is applicable to the general direct-sequence spread spectrum system, our focus is mainly on its application to the CDMA forward link [11]. The detection and false alarm probabilities of the CDMA noncoherent demodulator are derived analytically by taking into account the correlation between successive demodulator outputs within the period of post-detection integration. Based on the detection performance derivation, numerical evaluations of the code acquisition performance shall be made to address the problems of selecting the design parameters for pilot signal acquisition in the CDMA forward link. The numerical evaluations also illustrate the effects of post-detection integration and signal fading on code acquisition performance. This paper is organized as follows. In section Ⅱ, the double-dwell serial code acquisition technique is described with the analytical derivation of the mean acquisition time. The detection performance of the CDMA noncoherent QPSK demodulator is derived in section Ⅲ in frequency-selective Rayleigh fading channel in terms of the probabilities of detection and

false alarm. In section Ⅳ, the numerical performance evaluations of the code acquisition technique are made for pilot signal acquisition in the CDMA forward link, followed by the conclusion in section Ⅴ.

Ⅱ. A Double-Dwell Serial Code Acquisition Technique

The block diagram of the double-dwell serial code acquisition technique is described in Figure 1. The technique employs two modes, the search and verification modes. The decision rule in each mode is given by the well-known hypothesis test based on Neyman-Pearson criterion [10]. The time required for each test in the search mode is defined as the first dwell time($\tau_{D,1}$), which should be set as short as possible enough to rapidly reject the H_0 hypotheses. Once the detector output in a given test cell exceeds a pre-determined threshold in the search mode, the test cell is

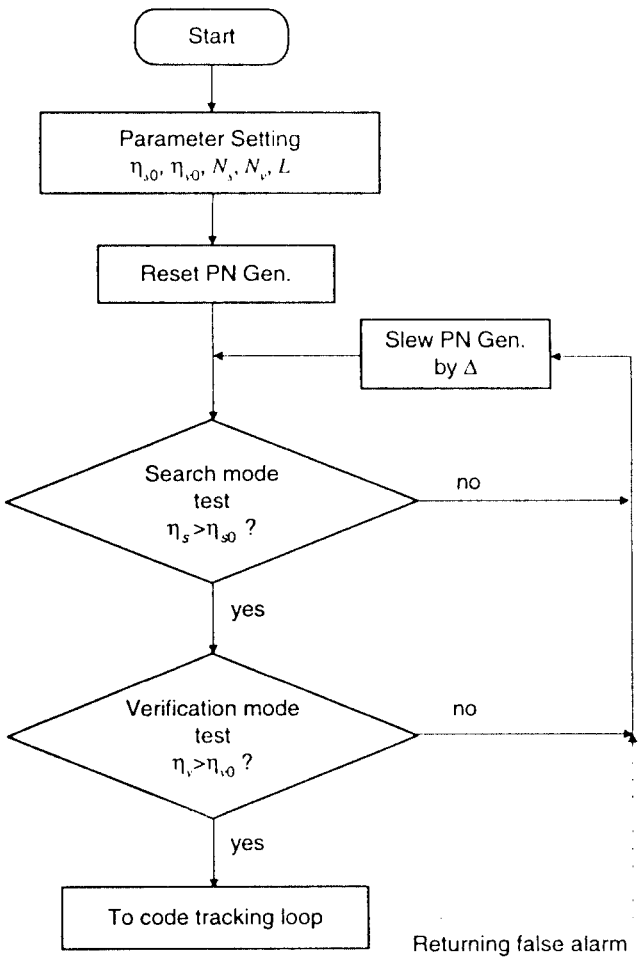

Figure 1. Block diagram of double-dwell serial code acquistion technique.

accepted tentatively as the H_1 cell, and the verification mode is activated to confirm whether the tentative H_1 decision is true or not. In order to provide a highly reliable decision in the verification mode, it is necessary not only to increase the period for coherent accumulation but also to take the sum of the successive correlator outputs as a decision variable, which means that the second dwell-time($\tau_{D,2}$) is significantly longer than the first dwell-time. If the H_1 decision is declared again in the verification mode, the correponding code phase shall be accepted as the true code phase of the incoming signal. Otherwise, the system rejects the test cell and the normal search mode is resumed from the next cell. In the catastrophic case where a H_0 cell pass the verification mode, it is assumed that the false alarm state is recognized in the tracking loop and the normal search mode is recommenced with the penalty time, $T_p(K_p\tau_{D,1})$ imposed, which is significantly large compared to the first or second dwell time.

The double-dwell serial code acquisition technique can be described by the circular state diagram as shown in Figure 2.a, where

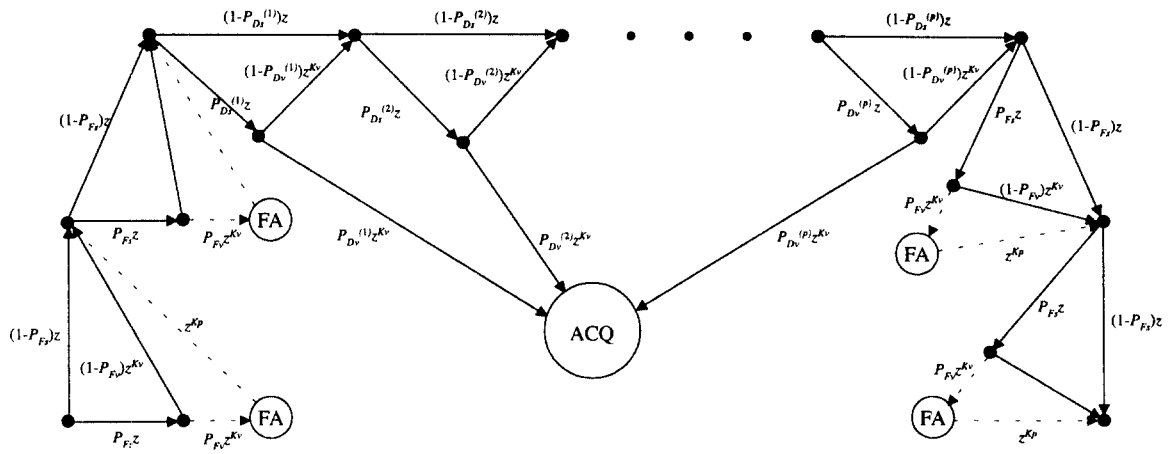

Figure 2a. State diagram

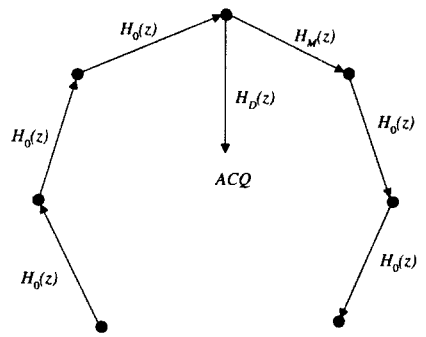

Figure 2b. Redueced state diagram.

the nodes on the outer and inner circles represent the test cells in the search and verification modes, respectively, with the dotted line denoting the returning false alarm state. In general, multiple cells (p-cells) belong to the H_1 region in frequency-selective fading channel, depending on the search step size. In the figure, $P_{Ds}^{(i)}$ and $P_{Dv}^{(i)}$ denote the probabilities that the i-th H_1 cell, $i = 1, 2, \ldots, p$, will be accepted in the search and verification modes, respectively. P_{Fs} and P_{Fv} represent the false alarm probabilities in the search and verification modes, respectively. The state diagram in Figure 2.a can be reduced to Figure 2.b by flow graph reduction method, where $H_0(z)$, $H_D(z)$, and $H_M(z)$ are given by

$$\begin{aligned} H_0(z) &= (1-P_{Fs})z + P_{Fs}(1-P_{Fv})z^{K_v+1} \\ &\quad + P_{Fs}P_{Fv}z^{K_v+K_p+1} \\ H_D(z) &= \sum_{j=1}^{p} P_{Ds}^{(j)}P_{Dv}^{(j)}z^{K_v+1}\prod_{i=1}^{j-1}\left[\left(1-P_{Ds}^{(i)}\right)z \right. \\ &\quad \left. + P_{Ds}^{(i)}\left(1-P_{Dv}^{(i)}\right)z^{K_v+1}\right] \\ H_M(z) &= \prod_{j=1}^{p}\left[\left(1-P_{Ds}^{(j)}\right)z + P_{Ds}^{(j)}\left(1-P_{Dv}^{(j)}\right)z^{K_v+1}\right]. \end{aligned} \tag{1}$$

From Mason's formula, the transfer function from a starting node which is i-branches counter-clockwise from the final destination node is

$$U_i(z) = \frac{H_0^{\,i}(z)H_D(z)}{1-H_M(z)H_0^{v-p}(z)}, \tag{2}$$

with v denoting the total number of test cells. Since all nodes are equally likely assuming that the starting node is outside the H_1 region, the total transfer function averaged over all v-p starting nodes is

$$U(z) = \frac{1}{v-p}\frac{H_D(z)}{1-H_M(z)H_0^{v-p}(z)}\sum_{i=1}^{v-p}H_0^{i}(z)$$

$$= \sum_{j=0}^{\infty} C_j z^j, \tag{3}$$

where $U(z)$ has the form of moment generating function with $C_j, j = 0, 1, \ldots, \infty$, representing the probability that the acquisition time will be $j \times \tau_{D,1}$. Therefore, the mean acquisition time is given by

$$E[T_{acq}] = \frac{dU(z)}{dz}\Big|_{z=1}\tau_{D,1}, \tag{4}$$

where $\left.\dfrac{dU(z)}{dz}\right|_{z=1} \approx$

$$\frac{(v-p)H_0(1)\{1+H_M(1)\}+2\{H_D'(1)+H_M'(1)\}}{2\{1-H_M(1)\}} \tag{5}$$

with

$$\begin{aligned} H_M(1) &= \prod_{j=1}^{p}\left(1-P_{Ds}^{(j)}P_{Dv}^{(j)}\right) \\ H_M'(1) &= \sum_{j=1}^{p}\left[\left(1-P_{Ds}^{(j)}\right)+\left(1+K_v\right)P_{Ds}^{(j)}\left(1-P_{Dv}^{(j)}\right)\right]\prod_{\substack{i=1\\ i\neq j}}^{p}\left(1\right. \\ &\quad \left. - P_{Ds}^{(i)}P_{Dv}^{(i)}\right) \\ H_D(1) &= \sum_{j=1}^{p}P_{Ds}^{(j)}P_{Dv}^{(j)}\prod_{i=1}^{j-1}\left(1-P_{Ds}^{(i)}P_{Dv}^{(i)}\right) \\ H_D'(1) &= \left(1+K_v\right)\sum_{j=1}^{p}P_{Ds}^{(j)}P_{Dv}^{(j)}\prod_{i=1}^{j-1}\left(1-P_{Ds}^{(i)}P_{Dv}^{(i)}\right) \\ &\quad + \sum_{j=2}^{p}P_{Ds}^{(j)}P_{Dv}^{(j)}\sum_{k=1}^{j-1}\left\{\left(1-P_{Ds}^{(k)}\right)+\left(1+K_v\right)P_{Ds}^{(k)}\right. \\ &\quad \left.\left(1-P_{Dv}^{(k)}\right)\right\}\prod_{\substack{i=1\\ i\neq k}}^{j-1}\left(1-P_{Ds}^{(i)}P_{Ds}^{(i)}\right) \end{aligned} \tag{6}$$

$H_0(1)=1$

$H'_0(1)=1+K_vP_{Fs}+K_pP_{Fs}P_{Fv}$.

Ⅲ. Detection and False Alarm Probabilities

A. Signal Modelling : The statistics of the

noncoherent QPSK demodulator output for synchronous CDMA system is discussed in the Appendix in frequency-selective Rayleigh fading channel, over which q-multipath signals are assumed to arrive at receiver with different time delays. Under H_1 hypothesis, where the timining errors between the local PN generator and the received signals are less than one PN chip, the I/Q channel outputs are written again

$$Y_I = N\sqrt{E_{c,p}}\sum_{k=1}^{q}\alpha_k R(\tau_k)\cos\varphi_k + n_{I,N}$$
$$Y_Q = N\sqrt{E_{c,p}}\sum_{k=1}^{q}\alpha_k R(\tau_k)\sin\varphi_k + n_{Q,N}. \quad (7)$$

While the variances of the I/Q channel noises are functions of α_k and τ_k in the CDMA forward link, we may ignore their dependency and assume that I/Q channel noises are Gaussian, independent of each other since our analysis focuses on the worst case where the mobile locates near the cell boundary. In addition, it is also assumed that the randomness of α_k affects only the signal component with Rayleigh fading characteristics. These assumptions seem reasonable near the cell boundary where many noise components with independent fading characteristics contribute to the I/Q stationary noise components with variances $I_0/2$. In this case, considering the randomness of α_k, the mean of Z is given by

$$\begin{aligned} E[Z] &= E\left[Y_I^2 + Y_Q^2\right] \\ &= N^2 E_{c,p}\sum_{k=1}^{q}E[\alpha_k^2]R^2(\tau_k) + NI_1 \\ &= V_S + V_N \\ &= V_F, \end{aligned} \quad (8)$$

with

$$\begin{aligned} I_1 &= N_o + I_{oc} + I_{dc}\sum_{k=1}^{q}\alpha_k^2\left\{1 - R^2(\tau_k)\right\} \\ &\approx I_0. \end{aligned} \quad (9)$$

In the above equation, N_o, I_{oc}, and I_{dc} are the noise spectral densities due to the background noise, the interferences from other cells and the desired cell, respectively, in case where the signals are out of synchronization with the sequence of the local PN generator. Under H_0 hypothesis, the noise variance is given by

$$I_0 = N_0 + I_{oc} + I_{dc}. \quad (10)$$

B. Detection Performance in the Search Mode

: Since the H_0 cells should be rejected as rapidly as possible in the search mode, the post-detection integration for improving the detection performance is not necessary. Although the optimal decision rule for the noncoherent detector based on Neyman-Pearson criterion is the log-likelihood ratio test [12], the sub-optimal decision rule which takes the detector output energy as a decision variable is widely accepted due to its convenience in implementation. The decision rule in this case is given by

$$\eta_s = Z_s \rangle \eta_{s0}, \quad (11)$$

where the subscript 's' has been used to denote the search mode processing and η_{s0} is a decision threshold in the search mode. For rapid rejection of H_0 cells, it may be desirable to take the accumulation period as short as possible, corresponding to the period of Walsh sequence. Under H_0 hypothesis, since η_s has the mean of $V_{Ns}=N_sI_0$, with Ns denoting the number of accumulated PN chips in the search mode, the random variable $2\eta_s/V_{Ns}$ has a χ^2 distribution with 2 degrees of freedom. The probability density function (pdf) of η_s is

therefore given by

$$f_{\eta_s}(\eta_s|H_0)=\frac{1}{V_{Ns}}\exp(-\eta_s/V_{Ns}), \tag{12}$$

and the probability of false alarm in the search mode is

$$\begin{aligned}P_{Fs}&=\int_{\eta_{s0}}^{\infty} f_{\eta_s}(\eta_s|H_0)\,d\eta_s\\&=\exp(-\eta_{s0}/V_{Ns}).\end{aligned} \tag{13}$$

Under H_1 hypothesis, the mean of Z_s is given by

$$\begin{aligned}E[Z_s]&=N_s^2E_{c,p}\sum_{k=1}^{q}E[\alpha_k^2]R^2(\tau_k)+N_sI_1\\&\approx V_{Ss}+V_{Ns}\\&=V_{Fs}.\end{aligned} \tag{14}$$

Thus, the pdf of η_s is

$$f_{\eta_s}(\eta_s|H_1)=\frac{1}{V_{Fs}}\exp(-\eta_s/V_{Fs}), \tag{15}$$

and the detection probability in the search mode is

$$\begin{aligned}P_{Ds}&=\int_{\eta_{s0}}^{\infty} f_{\eta_s}(\eta_s|H_1)\,d\eta_s\\&=\exp(-\eta_{s0}/V_{Fs}).\end{aligned} \tag{16}$$

C. Detection Performance in the Verification Mode : In order to provide a highly reliable decision in the verification mode, it may be necessary not only to increase the period for coherent accumulation but also to take the sum of the successive correlator outputs as a decision variable. The decision rule in the verification mode is therefore given by

$$\eta_v=\sum_{l=1}^{L}Z_{v,l}>\eta_{v0}, \tag{17}$$

where η_{v0} is a decision threshold in the verification mode. The subscript 'v' denotes the verification mode processing. L is the number of post-detection integration for improving the detection performance and $Z_{v,l}$, l=1, 2, ..., L, are the correlator outputs accumulated over the period of $N_v(mN_s)$ PN chips with m an integer. Under H_0 hypothesis, since the mean of $Z_{v,l}$ is V_{Nv}, the pdf of η_v is

$$f_{\eta_v}(\eta_v|H_0)=\frac{\eta_v^{L-1}}{(L-1)!V_{Nv}^{L}}\exp(-\eta_v/V_{Nv}), \tag{18}$$

and the probability of false alarm in the verification mode is given by

$$\begin{aligned}P_{Fv}&=\int_{\eta_{v0}}^{\infty} f_{\eta_v}(\eta_v|H_0)d\eta_v\\&=\exp(-\eta_{v0}/V_{Nv})\sum_{k=0}^{L-1}\frac{(\eta_{v0}/V_{Nv})^k}{k!}.\end{aligned} \tag{19}$$

We now derive the probability of detection in the verification mode by taking into account the correlation between successive demodulator outputs $Z_{v,l}$, l=1, 2, ..., L. Define a complex random vector $\mathbf{x}$ whose elements consist of I/Q channel outputs, each corresponding to the real and imaginary parts of the complex random variable x_l, l=1, 2, ..., L, respectively. That is,

$$\mathbf{x}=[x_1, x_2, \cdots, x_L]^T, \tag{20}$$

where superscript 'T' denotes the transpose operator. Then, the covariance matrix of $\mathbf{x}$ can be represented as

$$\begin{aligned}R_x&=E[\mathbf{x}\mathbf{x}^H]\\&=\mathbf{R}_s+V_{Nv}\mathbf{I},\end{aligned} \tag{21}$$

where $\mathbf{R}_s$ is the signal covariance matrix. The decision variable can be rewritten as

$$\eta_v=\mathbf{x}^H\mathbf{x}, \tag{22}$$

where the random variable η_v has a quadratic form of the Gaussian random vector $\mathbf{x}$. Define a random vector $\mathbf{y}=\mathbf{R}_x^{-1/2}\mathbf{x}$, then

$$E[yy^H]=\mathbf{R}_x^{-1/2}E[\mathbf{x}\mathbf{x}^H]\mathbf{R}_x^{-1/2}$$
$$=\mathbf{I}_L, \quad (23)$$

where $\mathbf{I}_L$ denotes the $L\times L$ identity matrix and $\mathbf{y}$ is a zero mean complex Gaussian random vector whose covariance matrix is an identity matrix. Thus, the decision variable is equivalently expressed as follow,

$$\eta_v=\mathbf{y}^H\mathbf{R}_x\mathbf{y}$$
$$=\sum_{l=1}^{L}\lambda_l|\omega_l|^2, \quad (24)$$

where $\omega_l=\mathbf{u}_l^H\mathbf{y}$, $l=1, 2, \ldots, L$, are Gaussian random variables with the same unit variance, independent of each other. λ_l and $\mathbf{u}_l$ are the l-th eigenvalue and eigenvector of $\mathbf{R}_x$, respectively. Since $\mathbf{R}_x$ is positive definite, the eigenvalues are always positive. The pdf of η_v may be easily derived by using the characteristic function of η_v, which is given by

$$\Phi(t)=E[e^{jt\eta_v}]$$
$$=\prod_{l=1}^{L}\left(1-jt\lambda_l\right)^{-1}. \quad (25)$$

In a general case of repeated eigenvalues where $\lambda_1>\lambda_2, \ldots, \lambda_k>\lambda_{k+1}=\lambda_{k+2}=, \ldots, =\lambda_L\geq V_{Nv}$, the characteristic function can be expressed as

$$\Phi(t)=\sum_{l=1}^{k}\frac{b_l}{1-j\lambda_l t}+\sum_{l=k+1}^{L}\frac{b_l}{\left(1-j\lambda_{k+1}t\right)^{l-k}}, \quad (26)$$

where

$$b_l=\begin{cases}\dfrac{(\lambda_l)^{L-1}}{(\lambda_l-\lambda_{k+1})^{L-k}}\displaystyle\prod_{\substack{i=1\\ i\neq l}}^{k}(\lambda_l-\lambda_i)^{-1}, & \text{for } l=1, 2, \ldots, k\\ \dfrac{(-j\lambda_{k+1})^{l-L}}{(L-l)!}\dfrac{d^{(L-l)}}{dt^{(L-l)}}\left\{\left(1-j\lambda_{k+1}t\right)^{L-k}\Phi(t)\right\}\Big|_{t=\frac{1}{j\lambda_{k+1}}}, & \text{for } l=k+1, k+2, \ldots, L.\end{cases} \quad (27)$$

Thus, the pdf of η_v is given by

$$f_{\eta_v}(\eta_v|H_1)=\sum_{l=1}^{k}\frac{b_l}{\lambda_l}\exp(-\eta_v/\lambda_l)+$$
$$\sum_{l=k+1}^{L}\frac{b_l\eta_v^{l-k+1}}{(\lambda_{k+1})^{l-k}(l-k-1)!}\exp(-\eta_v/\lambda_{k+1}). \quad (28)$$

Finally, the detection probability is

$$P_{Dv}=\int_{\eta_{v0}}^{\infty}f_{\eta_v}(\eta_v|H_1)d\eta_v$$
$$=\sum_{l=1}^{k}b_l\exp(-\eta_{v0}/\lambda_l)+\exp(-\eta_{v0}/\lambda_{k+1})\sum_{l=k+1}^{L}b_l$$
$$\sum_{m=1}^{l-k}\frac{(\eta_{v0}/\lambda_{k+1})^{l-k-m}}{(l-k-m)!}.$$

Ⅳ. Numerical Results and Discussions

In this section, the performance of the code acquisition technique described in section Ⅱ is evaluated numerically, focusing on pilot signal acquisition in the CDMA forward link. The period of the I/Q PN sequences used for numerical evaluations is 2^{15} PN chips, where the PN chip rate is given by 1.2288 MHz. The search step size Δ is set to 1/2 T_c. The numbers of the PN chips for coherent accumulation in the search and verification modes are taken to be 64 and 256, respectively, that is, N_s=64 and N_v=256, assuming that the period of the Walsh sequence used for isolating the forward channels is 64 PN chips. The selection of N_v=256 may be reasonable for coherent accumulation in the verification mode considering the fading rate in real mobile communication environments. The tapped-delay line model shall be used for characterizing the frequency-selective Rayleigh fading channel, over which three signals are assumed to arrive at intervals of 1 PN chip. The energy of each signal is taken to be 0.57, 0.29, and 0.14 times the total pilot signal energy, respectively, which may be a typical example of the fading channel in

urban area. In this case, the number of H_i cells is 7. The Clarke's one dimensional model shall be also used for modelling the autocorrelation function of the faded signal, which can be expressed as

$$r_s(\tau)=J_o(2\pi f_m\tau), \tag{30}$$

where $J_0(\cdot)$ is the zero-order Bessel function of the first kind and $f_m=v/\lambda$ is the maximum Doppler spread with v and λ denoting the speed of mobile and the signal wavelength, respectively.

In usual, 20 % of the total transmit power of the CDMA cell site is devoted to the pilot signal [3]. Thus, unless specified otherwise, we take the pilot signal-to-noise ratio per PN chip (SNR_c) to be -11 dB, with the assumption that the interference from adjacent cells is around twice of that from the desired cell. In this case, the signal-to-noise ratios for each path are -13.4, -16.4, and -19.5 dB, respectively at τ=0. All numerical examples are given for the worst case where the minimum timing error is $\Delta/2$. Note that the signal energy in the detector output is proportional to $R^2(\tau)$. For the pulse shaping filter specified on IS-95, R(τ) may approximate to the sinc function

$$R(\tau)=\frac{\sin(\pi\tau/T_c)}{\pi\tau/T_c}. \tag{31}$$

Figure 3 shows the mean acquisition time for K_p = 500, L = 2, and f_m= 50 Hz. It is observed in the figure that the optimal decision thresholds normalized to noise variances in the search and the verification modes, respectively, are 3.0 and 8.7 for given conditions, and the corresponding mean acquisition time is 4.64 seconds. It is also observed that setting the decision thresholds significantly smaller or larger than optimal values in both modes greatly increases the mean acquisition time. Figures 4 and 5 illustrate the effect of post-detection integration on code acquisition performance for K_p = 500 and f_m= 50 Hz. The figures are X/Y sections of the three-dimen-

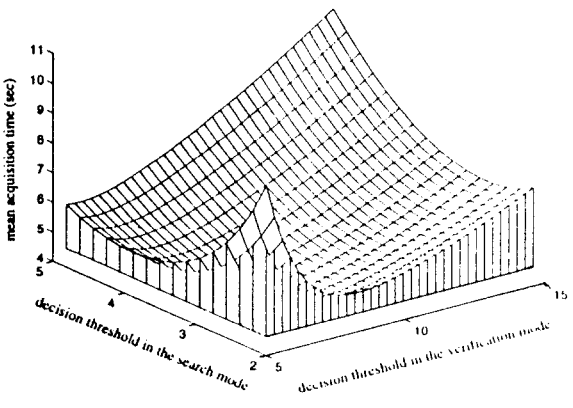

Figure 3. Mean acquisition time as a function of decision thresholds in the search and verification modes (SNR_c=-11 dB, L=2, N_s=64, N_v=256, f_m=50 Hz, and K_p=500).

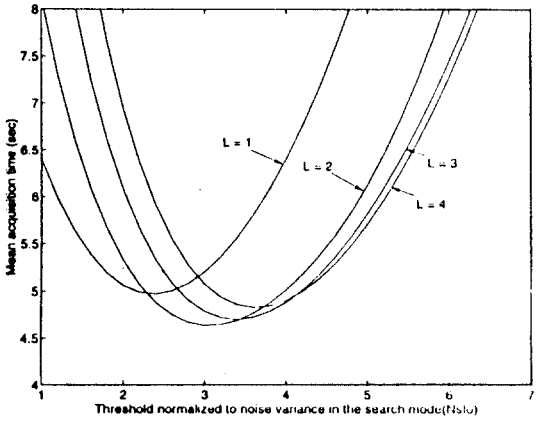

Figure 4. Mean acquisition time as a function of decision thresholds in the search mode (SNR_c=-11 dB, N_s=64, N_v=256, f_m=50 Hz, and K_p=500).

sional performance figures at the point of mininum mean acquisition time. It may be observed in the figures that while the minimum mean acquisition time does not depend significantly on the number of post-detection integration, L=2 or L=3 is optimal in terms of both the minimum mean acquisition time and the performance sensitivity to decision thresholds. Figure 6 illustrates the effect of signal fading on the acquisition performance for K_p = 500 and L=2. It is seen in the figure that as the maximum Doppler spread increases, the mean acquisition time decreases, which is simply due to the fact that the time diversity between successive demodulator outputs constituting the decision variable in the verification mode can be provided efficiently for higher Doppler spread. However, since the maximum Doppler spread due to the mobility of the subscriber is typically less than 200 Hz in real mobile communication environments, it may be said that signal fading does not affect the code acquisition performance seriously. Figure 7 illustrates the effect of delay spread on code acquisition performance. In the figure, 'FN' and 'FS' denote the frequency-nonselective and frequency-selective cases, respectively. It is shown in the figure that the frequency-nonselective case provides slightly better performance than frequency-selective case.

Ⅴ. Conclusion

In this paper, we have analyzed the performance of the double-dwell serial code acquisition technique for pilot signal acquisition in the CDMA forward link in frequency-selective Rayleigh fading channel. A general expression for the mean acquisition time has been derived by considering the multiple H_1 cells and returning false alarm. The detection and false alarm probabilities have been also derived analytically by taking into account the correlation between successive demodulator outputs within the period of post-detection integration. Based on the detection performance derived and the expression for the

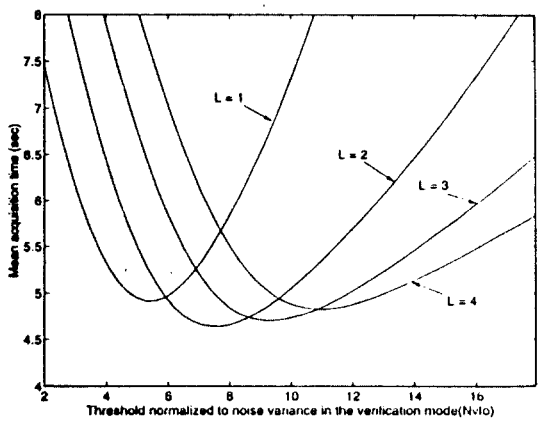

Figure 5. Mean acquisition time as a function of decision thresholds in the verification mode (SNR_c=-11 dB, N_s=64, N_v=256, f_m=50 Hz, and K_p=500).

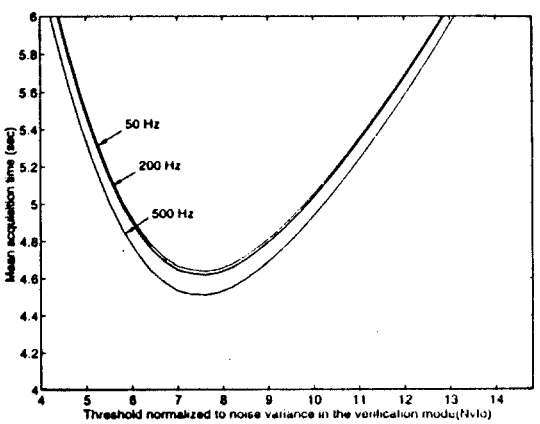

Figure 6. Effect of signal fading on mean acquistion time (SNR_c=-11 dB, L=2, N_s=64, N_v=256, and K_p=500).

mean acquisition time, the code acquisition performance has been evaluated numerically for pilot signal acquisition in the CDMA forward link.

It has been observed from numerical evaluations that while the minimum mean acquisition time does not depend significantly on post-detection integration, L=2 or 3 provides best performance in terms of both the mean acquisition time and the performance sensitivity to decision thresholds. The example for evaluating the effect of signal fading illustrates that the fading rate hardly affect the code acquisition performance in real mobile communication environments, which is due mainly to the fact that the time diversity between successive demodulator outputs constituting the decision variable in the verification mode is not provided efficiently within a practical range of fading rate.

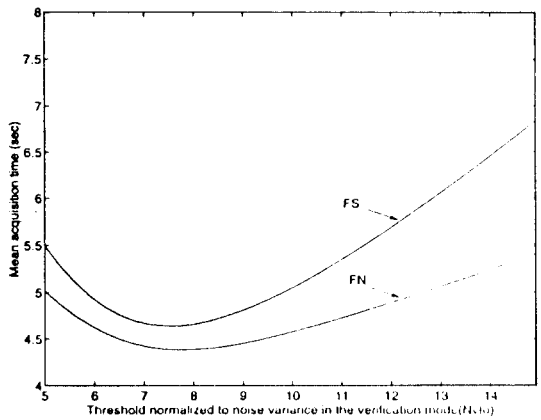

Figure 7. Effect of delay spread on mean acquistion time (SNR_c=-11 dB, L=2, N_s=64, N_v=256, f_m=50Hz, and K_p=500).

Appendix. Statistics of Noncoherent QPSK Demodulator Output in Synchronous CDMA System

We herein discuss the statistics of noncoherent QPSK demodulator output in synchronous CDMA system such as CDMA forward link in frequency-selective Rayleigh fading channel. A balanced QPSK demodulator for pilot signal acquisition/demodulation is depicted in Figure 8. To begin with, we first consider the single cell case and then extend the results for a multi-cell case. The tapped-delay line model shall be used for characterizing the fading channel, over which q-signals are assumed to arrive at mobile with different time delays.

The transmitted signal from the base station can be written as

$$s(t)=\left[\sqrt{E_{c,p}}\sum_{m}a_{I,m}h(t-mT_c)+\sum_{j=1}^{N_s}\sqrt{E_c^{(j)}}\right.$$

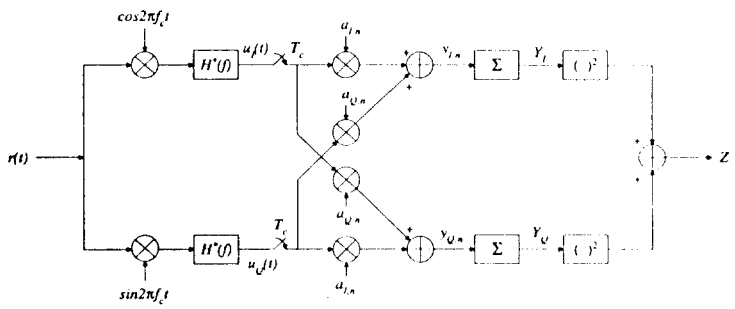

Figure 8. Simplified CDMA noncoherent QPSK demodulator.

$$\sum_m x_m^{(j)} W_m^{(j)} a_{I,m} h(t-mT_c)\Big]\cos(2\pi f_c t) + \Big[\sqrt{E_{c,p}}\sum_m a_{Q,m} h(t-mT_c) + \sum_{j=1}^{N_u}\sqrt{E_c^{(j)}} \sum_m x_m^{(j)} W_m^{(j)} a_{Q,m} h(t-mT_c)\Big]\sin(2\pi f_c t), \quad (32)$$

where $E_c^{(j)}$ represents the traffic signal energy per PN chip for the j-th user and $E_{c,p}$ denotes the pilot signal energy per PN chip. N_u, T_c, and $h(t)$ are the number of users, the PN chip duration, and the impulse response of the pulse shaping filter, respectively. $x_m^{(j)}$ is the information sequence which is constant within the period of Walsh sequence and $W_m^{(j)}$ is the Walsh sequence for isolating the channels. $a_{I,m}$ and $a_{Q,m}$ denote the I/Q PN sequences. Ignoring the signal attenuation due to the propagation loss, the received signal at mobile can be written as

$$r(t) = \sum_{k=1}^{q}\alpha_k\Big[\sqrt{E_{c,p}}\sum_m a_{I,m} h(t-mT_c+\tau_k) + \sum_{j=1}^{N_u}\sqrt{E_c^{(j)}} \sum_m x_m^{(j)} W_m^{(j)} a_{I,m} h(t-mT_c+\tau_k)\Big]\cos(2\pi f_c t+\varphi_k) + \sum_{k=1}^{q}\alpha_k\Big[\sqrt{E_{c,p}}\sum_m a_{Q,m} h(t-mT_c+\tau_k) + \sum_{j=1}^{N_u}\sqrt{E_c^{(j)}}\sum_m x_m^{(j)} W_m^{(j)} a_{Q,m} h(t-mT_c+\tau_k)\Big] \sin(2\pi f_c t+\varphi_k) + n_I(t)\cos(2\pi f_c t) - n_Q(t)\sin(2\pi f_c t), \quad (33)$$

where $n_I(t)$ and $n_Q(t)$ represent the narrowband Gaussian noise processes due to the background noise(or receiver thermal noise) each having a single-sided noise spectral density N_o. τ_k and α_k represent the relative time delay and the signal envelope. The I/Q channel outputs of the matched filter are

$$u_I(t) = \frac{1}{2}\sum_{k=1}^{q}\alpha_k\Big[\sqrt{E_{c,p}}\sum_m\Big\{\cos\varphi_k\, a_{I,m} + \sin\varphi_k\, a_{Q,m}\Big\} R(t-mT_c+\tau_k)\Big] + \frac{1}{2}\sum_{k=1}^{q}\alpha_k\Big[\sum_{j=1}^{N_u}\sqrt{E_c^{(j)}}\sum_m x_m^{(j)}\Big\{\cos\varphi_k W_m^{(j)} a_{I,m} + \sin\varphi_k W_m^{(j)} a_{Q,m}\Big\} R(t-mT_c+\tau_k)\Big] + \frac{1}{2}n_I'(t) \quad (34)$$

and

$$u_Q(t) = \frac{1}{2}\sum_{k=1}^{q}\alpha_k\Big[\sqrt{E_{c,p}}\sum_m\Big\{-\sin\varphi_k a_{I,m} + \cos\varphi_k a_{Q,m}\Big\} R(t-mT_c+\tau_k)\Big] + \frac{1}{2}\sum_{k=1}^{q}\alpha_k\Big[\sum_{j=1}^{N_u}\sqrt{E_c^{(j)}}\sum_m x_m^{(j)}\Big\{\cos\varphi_k W_m^{(j)} a_{Q,m} - \sin\varphi_k W_m^{(j)} a_{I,m}\Big\} R(t-mT_c+\tau_k)\Big] - \frac{1}{2}n_Q'(t), \quad (35)$$

with $R(t)=h(t)*h(-t)=\int_{-\infty}^{\infty}|H(f)|^2\cos 2\pi f t\, df$. Sampling the outputs and then multiplying the I/Q PN sequences for the i-th path, we obtain

$$y_{I,n} = u_I(nT_c)a_{I,n} + u_Q(nT_c)a_{Q,n} = \frac{1}{2}\sum_{k=1}^{q}\alpha_k\sum_m\Big\{\Big(\sqrt{E_{c,p}} + \sum_{j=1}^{N_u}\sqrt{E_c^{(j)}}x_m^{(j)}W_m^{(j)}\Big)\big(a_{I,m}a_{I,n} + a_{Q,m}a_{Q,n}\big)\Big\} R(nT_c - mT_c + \tau_k)\cos\varphi_k$$

$$+\frac{1}{2}\sum_{k=1}^{q}\alpha_k\sum_{m}\left\{\left(\sqrt{E_{c,p}}+\sum_{j=1}^{N_u}\sqrt{E_c^{(j)}}x_m^{(j)}W_m^{(j)}\right)\right.$$
$$\left.\left(a_{Q,m}a_{I,n}-a_{I,m}a_{Q,n}\right)\right\}R\left(nT_c-mT_c+\tau_k\right)\sin\varphi_k$$
$$+\frac{1}{2}\left\{n_I'(nT_c)a_{I,n}-n_Q'(nT_c)a_{Q,n}\right\}, \tag{36}$$

and

$$y_{Q,n}=u_I(nT_c)a_{Q,n}+u_Q(nT_c)a_{Q,n}$$
$$=\frac{1}{2}\sum_{k=1}^{q}\alpha_k\sum_{m}\left\{\left(\sqrt{E_{c,p}}+\sum_{j=1}^{N_u}\sqrt{E_c^{(j)}}x_m^{(j)}W_m^{(j)}\right)\right.$$
$$\left.\left(a_{Q,m}a_{Q,n}+a_{I,m}a_{I,n}\right)\right\}R\left(nT_c-mT_c+\tau_k\right)\sin\varphi_k$$
$$+\frac{1}{2}\sum_{k=1}^{q}\alpha_k\sum_{m}\left\{\left(\sqrt{E_{c,p}}+\sum_{j=1}^{N_u}\sqrt{E_c^{(j)}}x_m^{(j)}W_m^{(j)}\right)\right.$$
$$\left.\left(a_{I,m}a_{Q,n}-a_{Q,m}a_{I,n}\right)\right\}R\left(nT_c-mT_c+\tau_k\right)\cos\varphi_k$$
$$+\frac{1}{2}\left\{n_I'(nT_c)a_{Q,n}+n_Q'(nT_c)a_{I,n}\right\}. \tag{37}$$

Given $x_n^{(j)}$, a_k, and φ_k, for j=1, 2, ..., N_u and k=1, 2, ..., q, the means and variances of the I/Q channel outputs are derived as follow with the assumption that the local PN generator is perfectly synchronized with the signal in the i-th path, that is, τ_i=0.

$$E\left[y_{I,n}\right]=\alpha_i\left[\sqrt{E_{c,p}}+\sum_{j=1}^{N_u}\sqrt{E_c^{(j)}}x_n^{(j)}W_n^{(j)}\right]R(0)\cos\varphi_i$$
$$E\left[y_{Q,n}\right]=\alpha_i\left[\sqrt{E_{c,p}}+\sum_{j=1}^{N_u}\sqrt{E_c^{(j)}}x_n^{(j)}W_n^{(j)}\right]R(0)\sin\varphi_i$$
$$\mathrm{var}(y_{I,n})=\sigma^2_{I,I}+\sigma^2_{MP,I}+\sigma^2_{N,I}=I_1/2 \tag{38}$$
$$\mathrm{var}(y_{Q,n})=\sigma^2_{I,Q}+\sigma^2_{MP,Q}+\sigma^2_{N,Q}=I_1/2$$

where $\sigma^2_{I,I}$, $\sigma^2_{MP,I}$, and $\sigma^2_{N,I}$ represent the spectral densities of the inter-chip interference, multi-path interference, and the background noise in the I-channel, respectively. With the simple mathematical manipulations, we may obtain

$$\sigma^2_{I,I}\approx\frac{1}{2}\alpha_i^2\left[E_{c,p}+\sum_{j=1}^{N_u}E_c^{(j)}\right]\sum_{\substack{m=-\infty\\ m\neq 0}}^{\infty}\left[R(mT_c)\right]^2$$
$$\sigma^2_{MP,I}\approx\frac{1}{2}\left[E_{c,p}+\sum_{j=1}^{N_u}E_c^{(j)}\right]\sum_{k\neq i}^{q}\alpha_k^2\sum_{m=-\infty}^{\infty}\left[R(mT_c+\tau_k)\right]^2$$
$$\approx\frac{1}{2}\left[E_{c,p}+\sum_{j=1}^{N_u}E_c^{(j)}\right]\sum_{k\neq i}^{q}\alpha_k^2$$
$$\sigma^2_{N,I}=\frac{1}{2}N_0\int_{-\infty}^{\infty}|H(f)|^2df$$
$$=\frac{1}{2}N_0, \tag{39}$$

with the pulse shaping filter normalized, that is,

$$R(0)=\int_{-\infty}^{\infty}|H(f)|^2df=1. \tag{40}$$

Similarly, we obtain

$$\sigma^2_{I,Q}\approx\frac{1}{2}\alpha_i^2\left[E_{c,p}+\sum_{j=1}^{N_u}E_c^{(j)}\right]\sum_{\substack{m=-\infty\\ m\neq 0}}^{\infty}\left[R(mT_c)\right]^2$$
$$\sigma^2_{MP,Q}\approx\frac{1}{2}\left[E_{c,p}+\sum_{j=1}^{N_u}E_c^{(j)}\right]\sum_{k\neq i}^{q}\alpha_k^2$$
$$\sigma^2_{N,Q}=\frac{1}{2}N_0. \tag{41}$$

Therefore, $y_{I,n}$ and $y_{Q,n}$ can be modelled as

$$y_{I,n}=\alpha_i\left[\sqrt{E_{c,p}}+\sum_{j=1}^{N_u}\sqrt{E_c^{(j)}}x_n^{(j)}W_n^{(j)}\right]\cos\varphi_i+n_{I,n}$$
$$y_{Q,n}=\alpha_i\left[\sqrt{E_{c,p}}+\sum_{j=1}^{N_u}\sqrt{E_c^{(j)}}x_n^{(j)}W_n^{(j)}\right]\sin\varphi_i+n_{Q,n}, \tag{42}$$

where $n_{I,n}$ and $n_{Q,n}$ are the samples of the lowpass-filtered noise processes with variance

$I_1/2$. It should be noted that the I/Q noise variances are the function of α_k, k=1, 2, ..., q and τ_i. After coherent accumulation over the period of N-PN chips, where N is an integer multiple of the period of the Walsh sequence, the deterministic terms in the bracket resulting from N_u users are all cancelled due to the orthogonality property of the Walsh function. In this case, Y_I and Y_Q have means and variances,

$$E\left[Y_I=\sum_{n=1}^{N} y_{I,n}\right]=\alpha_i N\sqrt{E_{c,p}}\cos\varphi_i$$
$$E\left[Y_Q=\sum_{n=1}^{N} y_{Q,n}\right]=\alpha_i N\sqrt{E_{c,p}}\sin\varphi_i$$
$$\mathrm{var}(Y_I)=\mathrm{var}(Y_Q)=NI_1/2. \tag{43}$$

Therefore, Y_I and Y_Q can be represented as,

$$Y_I=\alpha_i N\sqrt{E_{c,p}}\cos\varphi_i+n_{I,N}$$
$$Y_Q=\alpha_i N\sqrt{E_{c,p}}\sin\varphi_i+n_{Q,N}. \tag{44}$$

The above equation has been derived with the assumption that the sequence of the local PN generator has been synchronized perfectly with the signal in the i-th path and out of synchronization with the signals in the k-th path ($k\neq i$)for a single cell case. In the more general case where there is a timing error τ_k between the local PN generator and the signal in the k-th path, the I/Q channel outputs due to the q-multipath signals are

$$Y_I=N\sqrt{E_{c,p}}\sum_{k=1}^{q}\alpha_k R(\tau_k)\cos\varphi_k+n_{I,N}$$
$$Y_Q=N\sqrt{E_{c,p}}\sum_{k=1}^{q}\alpha_k R(\tau_k)\sin\varphi_k+n_{Q,N}, \tag{45}$$

with

$$R(\tau_k)\approx 0, \quad \text{for } |\tau_k|>T_c. \tag{46}$$

In this case, I_1 is given by

$$I_1=N_o+I_{oc}+I_{dc}\sum_{k=1}^{q}\alpha_k^2\left\{1-R^2(\tau_k)\right\}, \tag{47}$$

where I_{oc} and I_{dc} represent the interference spectral densities resulting from other cells and the desired cell, respectively, when the local PN generator is out of synchronization with all of the input signals. In this case, I_{dc} is given by

$$I_{dc}=E_{cp}+\sum_{j=1}^{N_s}E_c^{(j)}. \tag{48}$$

References

1. W. C. Y. Lee, "Overview of cellular CDMA," *IEEE Trans. on Vehicular Technology*, vol. 40, No. 2, pp.291~302, May. 1991.
2. R. L. Pickholtz, L. B. Milstein, and D. L. Schilling, "Spread spectrum for mobile communications," *IEEE Trans. on Vehicular Technology*, vol. 40, No. 2, pp.313~322, May. 1991.
3. K. S. Gilhousen, I. M. Jacobs, R. Padovani, A. J. Viterbi, L. A. Weaver, and C. E. Wheatly, "On the capacity of a cellular CDMA system," *IEEE Trans. onVehicular Technology*, vol. 40, No. 2, pp.303~312, May. 1991.
4. A. Polydoros and C. L. Weber, "A unified approach to serial search spread-spectrum code acquisition - part I and II ," *IEEE Trans. on Commun.*, vol. COM-32, No. 5, pp.265-283, May, 1984.
5. J. K. Holmes and C. C. Chen, "Acquisition time performance of PN spread-spectrum systems," *IEEE Trans. on Commun.*, vol. COM-25, No. 8, pp.778~784, August. 1977.
6. H. R. Park and B. J. Kang, "On serial search code acquisition for direct-sequence spread spectrum system : An application to IS-95 CDMA system," *Proceedings of IEEE Vehicular*

Technology Conference, Rosemont, Illinois, USA, 26~28 July, 1995.

7. D. M. Dicarlo and C. L. Weber, "Statistical performance of single dwell serial synchronization systems," *IEEE Trans. on Commun.*, vol. COM-28, No. 8, pp.1382~1388, August. 1980.
8. E. Sourour and S. C. Gupta, "Direct-sequence spread-sprectrum parallel acquisition in nonselective and frequency-selective and frequency-selective Rician fading channels," *IEEE Journal on Selected Areas in Communications*, vol. 10, No. 3, pp.535~544, April. 1992.
9. E. Sourour and S. C. Gupta, "Direct-sequence spread-sprectrum parallel acquisition in a fading mobile channel," *IEEE Trans. on Commun.*, vol. COM-38, No. 7, pp.992~998, July. 1990.
10. M. K. Simon, J. K. Omura, R. A. Scholtz, and B. K. Levitt, *Spread spectrum communications*, vol. III, Ch. 1, Computer Science Press, 1985.
11. *Telecommunications industry association/ Electronic industry association interim standard-95*, Ch. 5~7, July. 1993.
12. H. L. Van Trees, *Detection, estimation, and modulation theory*, Part I, Ch. 2, Wiley, 1968.

朴 亨 來(Hyung-Rae Park) 정회원

1960년 10월 25일생
1982년 2월 : 한국항공대학 전자공학과 졸업(학사)
1985년 8월 : 연세대학교 대학원 전자공학과 졸업(석사)
1993년 12월 : Syracuse Univ. 전자공학과 졸업(박사)
1985년 9월~현재 : 한국전자통신연구소 선임연구원
※주관심 분야 : 레이다신호처리 방향탐지, 디지탈통신, 대역확산통신 등

康 法 周(Bub-Joo Kang) 정회원

1961년 8월 20일생
1983년 2월 : 경희대학교 전자공학과 졸업(공학사)
1985년 8월 : 연세대학교 대학원 전자공학과 졸업(공학석사)
1992년 3월~현재 : 연세대학교 대학원 전자공학과 박사과정
1988년 2월~현재 : 한국전자통신연구소 선임연구원